

Mixing in circulating flows

M. Hari, R.B.H. Tan*

Department of Chemical Engineering, National University of Singapore, 10 Kent Ridge Crescent, Singapore 119260, Singapore

Received 13 June 1998; received in revised form 30 November 1998; accepted 20 December 1998

Abstract

A new model for mixing in circulatory flows has been developed. The model is conceptually simple and uses a single parameter γ (with values between -1 and 1) representing physical flow conditions in the circulation loop to simulate the different mixing behaviour ranging from perfect plug flow to complete backmixing. Model predictions of tracer concentration profiles and mixing times are in good agreement with the experimental results from tracer studies in an external loop airlift system. © 1999 Elsevier Science S.A. All rights reserved.

Keywords: Mixing; Circulatory flows; External loop; Airlift system; Tracer studies

1. Introduction

The study of fluid mixing is an important part of the successful design and scale up of any chemical process vessel. Indeed a major proportion of the processing time is taken up by the mixing process alone as the materials are passed through the process. Several excellent books have been published on the subject [1,2].

Circulatory flows occur in a significant class of mixers and contactors, including those with a well-defined circulation path (for example, two phase- and three phase-airlift reactors) and those with a less defined circulation path (for example, helical ribbon mixers). A commonly used approach in evaluating the mixing processes occurring in circulating flows is to calculate the mixing time and correlate it to the system parameters such as the circulation time. The concept of mixing time is based on the approach of the tracer response to steady-state conditions and is usually calculated as the time required to reach a specified degree of homogeneity. Numerous authors have assumed an exact correspondence between the circulation time (θ_c) and the peak-to-peak time (θ_{pp}), and based their experimental results and interpretation on that assumption [1–3].

Modelling of the mixing processes occurring in circulating flows has traditionally been based on the axial dispersion model. In this model, the important parameter is the Bodenstein number (Bo). An increase in Bo means that the “plug

flow” tends to dominate the mixing process. Recently, Dhaouadi et al. [4] have modelled the liquid phase mixing process in an external loop airlift reactor by assuming the flow in the riser to be plug flow with axial dispersion, that in the downcomer to be plug-flow and the disengagement tank and flow reversal sections to be continuous stirred tanks (CST) with and without bubbles, respectively. Gavrilescu and Tudose [5] have studied the liquid phase mixing of external loop airlift reactors in terms of the axial dispersion and the mixing time. They have proposed a simple correlation between the specific mixing time and the operating and geometrical parameters of the reactor.

Another approach is to recognise that the circulating flows belong to a class of flows known as suspended flows. The axiomatic and mathematical framework for such types of flow were developed by Bowen and Ruelle [6] and later simplified by Mazer [7]. Tan [8] and Mazer [9] recognised the value of such a treatment in describing the process of mixing in circulating flows. Tan [8] analysed the case of an ideal circulation mixer for laminar flow of a Newtonian fluid. Mazer [9] extended this case to include what he termed, rather confusingly, a well-mixed region. Both authors had stressed that it was important to distinguish between circulation time and peak-to-peak time, as both were not necessarily equal.

This paper builds on the concepts described by Tan [8] and Mazer [9] to develop a mixing model for a typical circulating flow system, namely an external loop airlift system. The predicted results from the model are then compared with experimental data from an external loop airlift reactor.

*Corresponding author. Tel.: +65-874-6360; fax: +65-779-1936; e-mail: chetanbh@nus.edu.sg

2. Description of model

2.1. Model equations

Consider a flow situation in which the fluid elements recirculate in one direction only through a two-dimensional surface $B(x)$, called the base space. Fluid elements passing through a point x on the base space will have a circulation time $g(x)$ before they return to the base space. This time can also be called the return time.

In many cases of typical interest, the dimensions of the circulation flow path length are much larger than that of the corresponding cross section and it would be reasonable to assume the existence of a well-mixed base space so that the model does not consider inhomogeneities in the x -direction but rather allows us to consider the inhomogeneities in the y -direction only. Mathematically, we have

$$\int_0^1 g(x) dx = 1. \quad (1)$$

Provided that the time is expressed in terms of the average circulation time, the integral represents the average circulation time as well as the volume of the mixer. Normalisation of these quantities gives us a basis for the comparison of the mixing rates resulting from different functions $g(x)$.

Let $f(x,y,t)$ represent the concentration at the point (x,y) and at the time t in which the value of the function changes according to the dynamics of the simplified suspended flow. Physically, $f(x,y,t)$ would represent the concentration of a tracer injected into the circulating flow system. At the base plane where there is complete mixing, we have

$$f(x, 0, t) = \int_0^1 f(s, g(s), t) ds, \quad (2)$$

$$f(x, y, t) = f(x, 0, t - y), \quad t - y \geq 0, \quad (3)$$

$$f(x, y, t) = f(x, y - t, 0), \quad t - y < 0. \quad (4)$$

Since the concentration at the base space is independent of x , we follow Mazer [9] in our approach for further simplification of the model. As pointed out earlier, inhomogeneities in x are eliminated and only the concentrations that are independent of x are propagated vertically upward. It is reasonable to consider only initial functions $f(x,y,0)$ that are independent of x . This allows us to collapse the two-dimensional model onto the y -axis and essentially reduces the problem to a one-dimensional transient case.

Applying the inverse function theorem and a change of variables to Eq. (2), the one-dimensional transient equations describing the evolution of the concentration function $f(y,t)$ are

$$f(0, t) = \int_{g(1)}^{g(0)} f(y, t) m(y) dy, \quad (5)$$

$$f(y, t) = f(0, t - y), \quad t - y \geq 0, \quad (6)$$

$$f(y, t) = f(t - y, 0), \quad t - y < 0. \quad (7)$$

The function $m(y)$ is referred to as the feedback measure. It is the derivative of the inverse of the roof function. Formally, we have

$$w(y) = \begin{cases} g^{-1}(y), & y \geq g(1), \\ 1, & y \leq g(1) \end{cases} \quad (8)$$

and

$$m(y) = -dw/dy, \quad g(1) \leq y \leq g(1), \quad (9)$$

where $g^{-1}(y)$ denotes the inverse of the roof function $g(x)$ and $w(y)$ is referred to as the weight function for the circulating flow.

Eq. (5)–Eq. (9) form the basis of the so-called circulating feedback model and they can be solved for the case of an ideal laminar flow circulation mixer as shown in Fig. 1. By injecting a known volume and concentration of some tracer into the circulation system, we can represent this as the initial condition, and Eq. (3) can be solved to yield the value of the concentration of the tracer at some position y and time t .

The velocity profile is given by

$$u(r) = u_c(1 - (r/R)^2), \quad (10)$$

where u_c is the centre line fluid velocity and r is measured from the centre line. It is readily shown that for the velocity profile given above, the corresponding weight function is

$$w(y) = \begin{cases} 1/4y^2, & y \geq 0.5, \\ 1, & y \leq 0.5. \end{cases} \quad (11)$$

The feedback measure is obtained by differentiating the weight function $w(y)$.

2.2. Mixing in an external loop airlift system

Gas–liquid airlift systems provide a practical example of a simple circulating flow. A typical external loop airlift reactor, shown schematically in Fig. 1, consists of a U-tube filled with liquid. Gas, sparged into one of the vertical sections of the U-tube, causes the liquid to circulate upward in this leg (the “riser”) and downwards in the other leg (the “downcomer”) due to the nett density difference between the two legs (the so-called gaslift or airlift action).

A disengagement tank located above the U-tube allows the gas bubbles from the riser to leave the system. It is usual to operate the system with total disengagement, i.e., no entrainment of gas bubbles into the downcomer [10].

We modify the model for the ideal circulation mixer by representing the airlift reactor as consisting of three distinct mixing regions as shown in Fig. 1. Firstly, there is a well-developed liquid flow region in the downcomer, the smooth U-bend and part of the riser below the sparger. The flow in this region is identical to that in the ideal circulation mixer. Mixing in the axial direction is due to the radial liquid velocity profile in the tube. Secondly, there is a bubbly

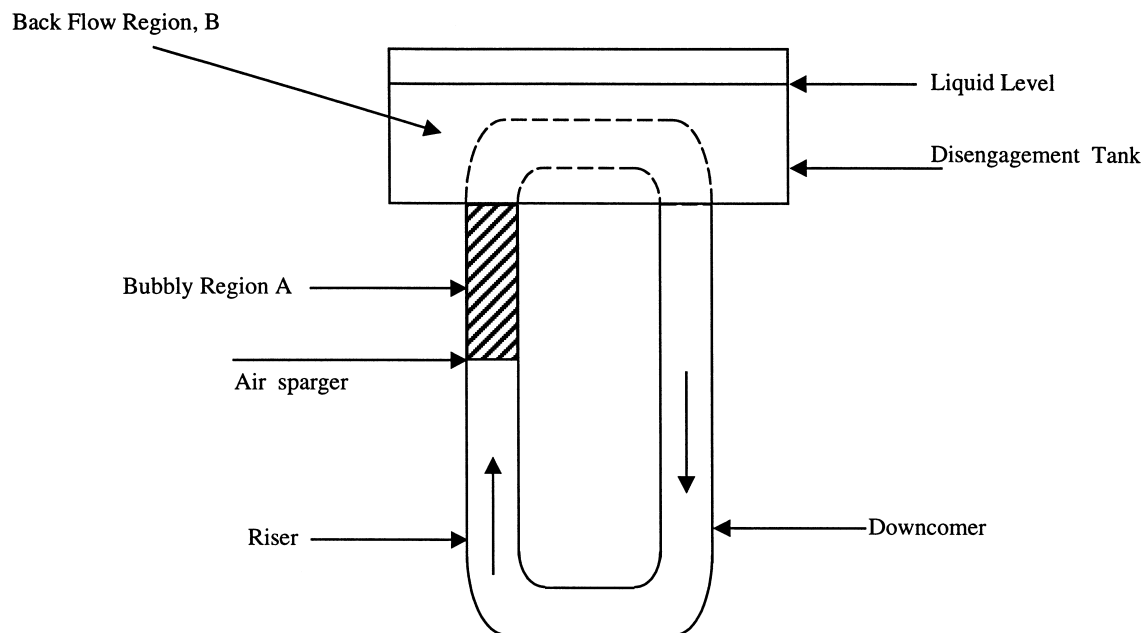


Fig. 1. Model representation of a U-tube airlift vessel.

region in the portion of the circulation path that is characterised by intense radial mixing due to the presence of unsteady bubbly flow. It is proposed to model the region as having complete mixing in the radial direction (equivalent to a flat velocity profile). Fluid in this region can therefore be visualised as being in “plug flow”. Mazer [9] considers the existence of such a region in his mathematical model but calls it rather confusingly, a “well-mixed” region. His simulation results clearly show that the contribution of this region is to reduce the extent of longitudinal mixing, as would be expected from the “plug flow” behaviour.

Thirdly, the disengagement tank is modelled as a back flow region. As depicted in Fig. 1, it is possible to visualise an ideal circulation loop by “completing the loop” formed by the U-tube. In the region of the disengagement tank, fluid in the idealised circulation loop is freely interchanged with fluid outside this loop (i.e., the backflow region). Physically, this represents conditions giving rise to “mixed flow”, i.e., the antithesis of “plug flow”. This would be equivalent to saying that the liquid in the disengagement tank, apart from the portion in the ideal loop, behaves essentially as a continuous stirred tank (CST) which accords with the approach by Merchuk and Yunger [11] and Dhaouadi et al. [4]. This picture is further supported by Russell et al. [12] who argue that the top section of the airlift reactor can be divided into two distinct zones, where the bulk of the recirculating liquid flows through a lower region (viz., the idealised circulation loop in our model), essentially bypassing an upper zone (which, in our case, is the CSTR zone). The only difference is that we model the two zones as having some degree of interaction.

Mathematically, we recall that the ideal circulation path has a volume normalised to unity. The volume occupied by

the bubbly region (A) can then be represented as a fraction, γ_A , which has values in the range 0–1.

In accordance with our view of the backflow region (B), as the antithesis of the bubbly (“plug flow”) region, we choose to model this region as effecting a reduction in γ_A .

Noting that region B is external to the circulation loop, the magnitude of this effect can be expressed by another parameter γ_B . We define a critical volume (V_c) corresponding to a zero value of γ_B . We can therefore calculate γ_B from

$$\gamma_B = (V - V_c)/V_c, \quad (12)$$

where $V \geq V_c$ and $\gamma_B \geq 0$. Then the nett circulation flow parameter, γ , is given by

$$\gamma = \gamma_A - \gamma_B, \quad (13)$$

where γ can take values in the range $-1 \leq \gamma \leq 1$. The circulation feedback model of Tan [8] can be easily extended to account for the parameter γ . The corresponding weight function is

$$w(y) = \begin{cases} [(1 - \gamma)/2(y - \gamma)]^2, & y \geq (1 + \gamma)/2, \\ 1, & y \leq (1 + \gamma)/2. \end{cases} \quad (14)$$

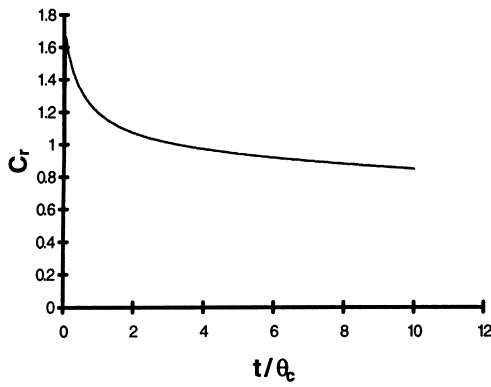
The transport equations for the circulation feedback model (Eq. (5)–Eq. (7)) can then be solved using this expression for $w(y)$.

3. Experimental

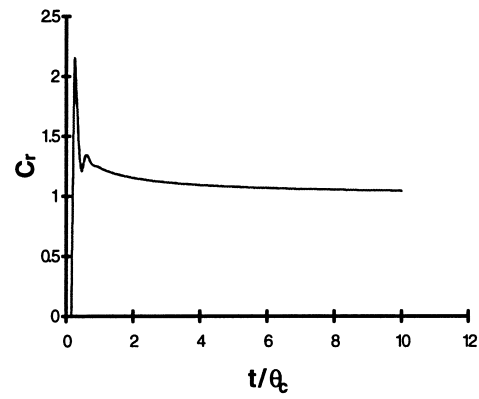
The airlift reactor used in our experimental studies had a total volume of approximately 5 l. The riser, downcomer and bottom flow reversal zones were constructed from 1 in nominal diameter PVC pipes. The length of the riser (or

downcomer) from the bottom of the gas disengagement tank was 0.88 m and the length of the bottom flow reversal zone was 0.185 m. The gas disengagement tank was rectangular in cross-section and had the dimensions of 0.29 m ×

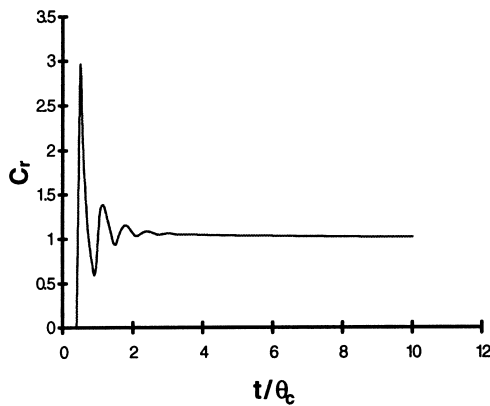
0.12 m × 0.12 m. Compressed air was sparged into the riser at a point 0.37 m from the bottom of the gas disengagement tank, using a perforated plate sparger. The range of superficial gas velocities used was from 0.0066 to 0.066 m s⁻¹.



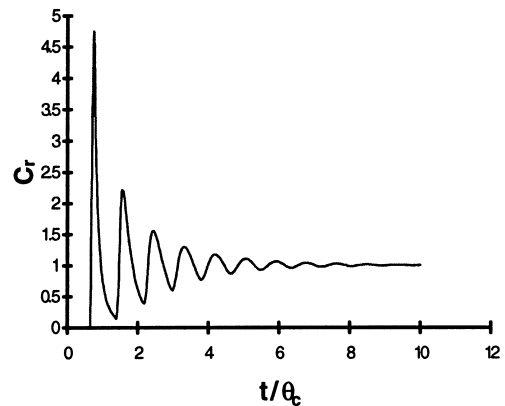
(a)



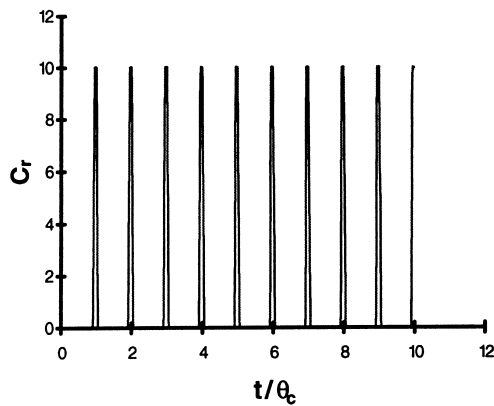
(b)



(c)



(d)



(e)

Fig. 2. Stimulated response curves for different values of γ : (a) $\gamma = -1.0$, (b) $\gamma = -0.5$, (c) $\gamma = 0$, (d) $\gamma = 0.5$ and (e) $\gamma = 1.0$.

Experiments were performed for four different liquid working volumes ranging from 1.8 to 2.5 l. For this experimental configuration the critical volume (V_c) was estimated to be 0.0018 m^3 . γ_A has the value of 0.171 and γ_B ranged from 0 to 0.39.

Conductivity probes (MicroElectrodes MI-900) were placed at two points 0.5 m apart in the right limb of the U-tube or the downcomer to detect the tracer (2 ml of 5 M NaCl solution) injected at the beginning of the downcomer. The electrodes are connected to the conductivity meters (Jenway 4010) which in turn are connected to a chart recorder (Yokogawa LR 4220) or a data-logging computer. The circulation times were calculated from the knowledge of the linear liquid velocity in the downcomer and the working vessel volume. It was also confirmed that the Reynolds number in the downcomer was largely within the laminar flow range.

4. Results and discussion

The numerical scheme of Tan [8] is applied to yield the dimensionless tracer concentration as a function of time and the simulations for $\gamma = -1, -0.5, 0, 0.5$ and 1 are shown in Fig. 2(a)–(e). The figures illustrate the various mixing behaviour possibilities ranging from perfect backmixing to plug flow.

Fig. 3(a)–(d) show the experimental response curves studied for four different working liquid volumes, namely 1.8, 2.0, 2.2 and 2.5 l, and a superficial gas velocity of 0.033 m s^{-1} . We have also plotted the simulated response curves using the simple model outlined earlier and corresponding values of the mixing parameter, γ . It can be seen that the model predicts the concentration profiles reasonably well.

The time between successive peaks, θ_{pp} , could be easily determined, and was found to be constant for each profile.

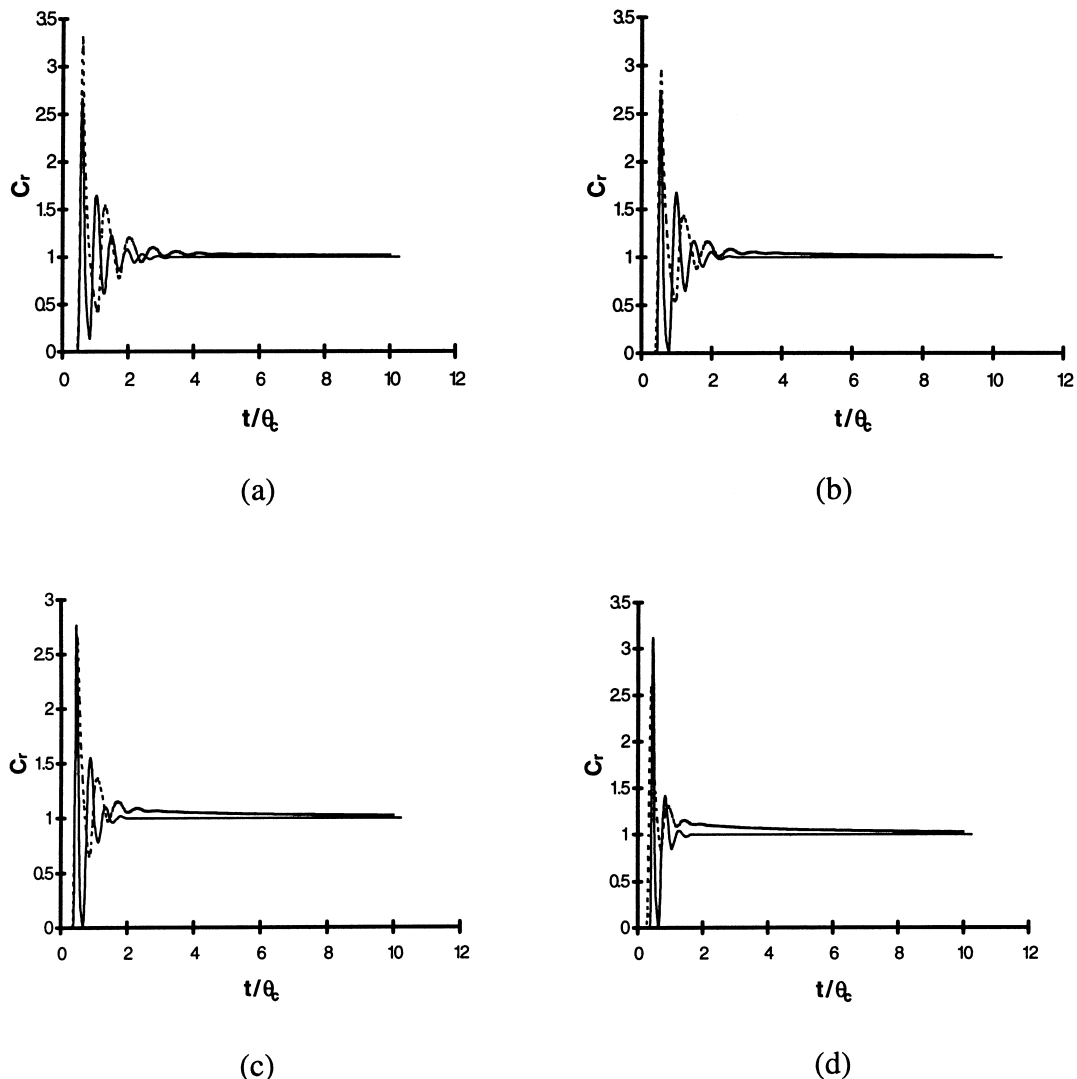


Fig. 3. Experimental (—) and predicted (---) response curve at $V_{sg}=0.033 \text{ m s}^{-1}$: (a) $V=1.8 \text{ l}$, $\gamma=0.1713$; (b) $V=2.0 \text{ l}$, $\gamma=0.0602$; (c) $V=2.2 \text{ l}$, $\gamma=-0.0509$; (d) $V=2.5 \text{ l}$, $\gamma=-0.2176$.

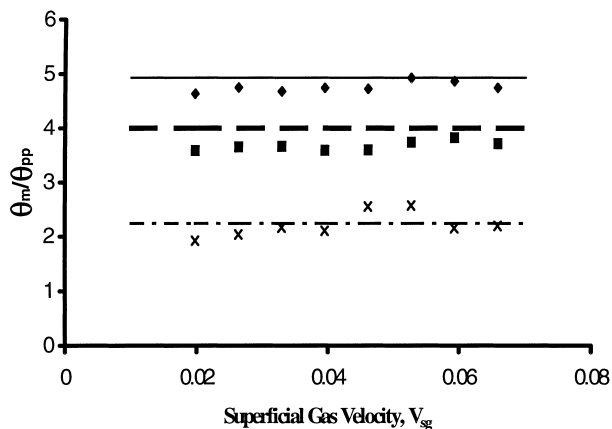


Fig. 4. Comparison of experimental and simulated values of θ_m/θ_{pp} : (◆) 1.8 l ($\gamma=0.1713$), (■) 2.0 l ($\gamma=0.0602$) \times 2.5 l ($\gamma=-0.2176$).

The ratio of θ_m (defined as the time required for the concentration of the tracer to reach within 5% of its steady-state value) to θ_{pp} generally indicates the rate of mixing and hence can be taken as a measure of mixing efficiency. Experimental values of θ_m/θ_{pp} are plotted on Fig. 4 versus gas superficial velocity for the liquid volumes of 1.8, 2.2 and 2.5 l. It appears that the variation of θ_m/θ_{pp} with gas flow rate is not appreciable, i.e., the ratio is fairly constant over the range of gas superficial velocities studied.

We also show in Fig. 4, the values of θ_m/θ_{pp} as predicted by our model using the corresponding values of γ . These values are constant for each γ , since the model is independent of the gas flow rate, provided the assumptions of “plug flow” behaviour in the bubbly region and of laminar flow in the downcomer remain approximately valid. These assumptions appear to be fully justified in the light of the experimental data. Overall, the evidence of Fig. 4 reveals the excellent agreement between model and experimental values of θ_m/θ_{pp} .

The range of values of θ_m/θ_{pp} also agree well with corresponding values for tracer studies in circulating flows reported by Nagata [1] and Tatterson [2] among others. The problem arises when these authors then equate θ_{pp} to θ_c , the average circulation time, and therefore assume that θ_m/θ_c is equivalent to θ_m/θ_{pp} . However, an inspection of Fig. 3(a)–(d) will reveal that θ_{pp} is not equal to θ_c . In fact, the ratio θ_{pp}/θ_c is in the range 0.4–0.6 for our experimental data. We recall that θ_{pp} is directly measured from the experimental response or theoretical curves, whereas θ_c is inferred from the ratio of the volume of vessel to the volumetric flow rate through an appropriately chosen cross-section. Clearly, the latter quantity, θ_c , equivalent to an average bulk circulation time, is based on hydrodynamic factors alone, whereas θ_{pp} would also be influenced by diffusional and convective mass transfer considerations. One would expect these quantities to be identical only in the ideal case of plug flow through out the entire vessel (as in the case illustrated by Fig. 2(e)).

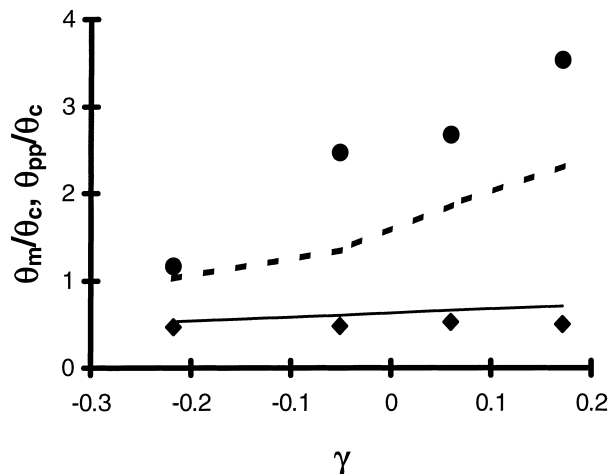


Fig. 5. Comparison of simulated and mean experimental values of θ_m/θ_c (—, simulated; ●, experimental) and θ_{pp}/θ_c (—, simulated; ◆, experimental) as a function of γ .

It is therefore recommended that existing correlations or expressions for θ_m as a function of θ_c be used with great care. It is essential to distinguish between θ_{pp} and θ_c in mixing studies involving interpretation of tracer response curves.

Finally Fig. 5 shows the simulated and average experimental values of θ_m/θ_c and θ_{pp}/θ_c as a function of γ . The agreement between the simulated and mean values of experimental data are good.

The new model for mixing should also be applicable to other circulatory flow systems such as helical ribbon mixers and conventional stirred tanks, where the value of the mixing parameter γ can be estimated from a knowledge of the geometry and physical nature of the flow. Further work is required in order to confirm the wider applicability of our model.

5. Conclusions

This paper presents a new model for mixing in circulating flows. The model relies on a single parameter, γ , which is directly related to the physical dimensions and conditions of the flow system. The model is validated against the experimental data for an external loop airlift vessel, and the results show very good agreement. Finally, the relationship between mixing time, θ_m , peak-to-peak time, θ_{pp} , and circulation time, θ_c , has been discussed and clarified.

6. Nomenclature

- Bo Bodenstein number (dimensionless)
- $B(x)$ two-dimensional base space
- C instantaneous tracer concentration (kmol m^{-3})

C_r	relative tracer concentration (dimensionless)
$f(x,y,t)$	concentration of the tracer at the position (x,y) and at time t (kmol m^{-3})
$g(x)$	distribution function of circulation times (or) roof function (s)
L	length of circulation flow path (m)
$m(y)$	feedback measure function
r	radius measured from the centreline (m)
R	radius of the circulation flow loop (m)
t	time (s)
u_c	centre-line velocity (m s^{-1})
$u(r)$	radial velocity profile (m s^{-1})
V	volume of fluid in reactor (m^3)
V_c	“critical” volume corresponding to a zero value of γ_B (m^3)
V_{sg}	superficial gas velocity (m s^{-1})
$w(y)$	weight function
x	point on the base space
y	distance from base space (m)

Greek symbols

γ	parameter in the circulation feedback model (dimensionless)
γ_A	volume fraction of the circulation flow loop representing the bubbly region (dimensionless)
γ_B	volume fraction representing the CST region (dimensionless)
θ_c	average circulation time (s)

θ_m	average mixing time (s)
θ_{pp}	average peak-to-peak time (s)

References

- [1] S. Nagata, *Mixing: Principles and Applications*, Kodansha, Tokyo, 1975.
- [2] G.B. Tatterson, *Fluid Mixing and Gas Dispersion in Agitated Tanks*, McGraw-Hill, New York, 1991.
- [3] P.R. Fields, N.K.H. Slater, Tracer dispersion in a laboratory airlift reactor, *Chem. Eng. Sci.* 38 (1983) 647–653.
- [4] H. Dhaouadi, S. Poncin, J.M. Hornut, G. Wild, P. Oinas, J. Korpijarvi, Mass transfer in an external-loop airlift reactor: experiments and modeling, *Chem. Eng. Sci.* 52 (1997) 3909–3917.
- [5] M. Gavrilescu, R.Z. Tudose, Mixing studies in external-loop airlift reactors, *Chem. Eng. J.* 66 (1997) 97–104.
- [6] R. Bowen, D. Ruelle, The ergodic theory of axiom A flows, *Invent. Math.* 79 (1975) 181–202.
- [7] A.A. Mazer, A model for investigating mixing speeds in suspended flows, *Physica D* 57 (1992) 226–237.
- [8] R.B.H. Tan, A novel approach to mixing in circulating flows, *Proceedings of the Asian Pacific Confederation of Chemical Engineers and Chemeca 93*, Melbourne, Australia, vol. 2, 1993, pp. 1–6.
- [9] A. Mazer, A model for investigating mixing times in circulation mixers, *Ind. Eng. Chem. Res.* 33 (1994) 871–877.
- [10] M.Y. Chisti, *Airlift Bioreactors*, Elsevier, Essex, 1989.
- [11] J.C. Merchuk, R. Yunger, The role of the gas–liquid separator of airlift reactors on the mixing process, *Chem. Eng. Sci.* 45 (1990) 2973–2975.
- [12] A.B. Russell, C.R. Thomas, M.D. Lilly, The influence of vessel height and top-section size on the hydrodynamic characteristics of airlift fermentors, *Biotechnol. Bioeng.* 43 (1994) 69–76.